ELSEVIER

Journal of Power Sources 109 (2002) 458–464

JOURNAL OF POWER SOURCES

www.elsevier.com/locate/jpowsour

Aluminum corrosion in electrolyte of Li-ion battery

S.S. Zhang*, T.R. Jow

US Army Research Laboratory, Adelphi, MD 20783, USA

Received 15 February 2002; accepted 1 March 2002

Abstract

The effect of lithium salt and electrolyte solvent on Al corrosion in Li-ion battery electrolytes was studied by using linear sweep voltammetry (LSV) and electrochemical impedance spectroscopy (EIS). The results showed that, in 1:1 (w/w) ethylene carbonate (EC)/1,2-dimethoxyethane (DME) solutions, the pitting potential of Al corrosion is about 3.2 V versus Li^+/Li, being independent of the type of salts. However, the salt has considerable impact on Al corrosion. Among the studied Li salts, the stability of Al with respect to the oxidative potentials was found to increase in an order of $CF_3SO_3Li < LiN(SO_2CF_3)_2 < LiClO_4 < LiPF_6 < LiBF_4$. We observed that a combination of two salts, such as $LiPF_6$ and CF_3SO_3Li, lowers the pitting potential and aggravates Al corrosion. Addition of compounds, which contain active fluoride, such as perfluoro-1-butanesulfonyl fluoride ($C_4F_9SO_2F$), into electrolytes can increase the pitting potential but cannot suppress Al corrosion.

Keywords: Li-ion battery; Current collector; Aluminum; Corrosion; Ac impedance

1. Introduction

In the state-of-the-art Li-ion technology, manufacturers and researchers use Al foil as a current collector for the cathode materials because it naturally forms a passive layer on the surface that helps it resist corrosion at high potentials. It was reported that, depending on environmental conditions, the naturally formed passive film on the Al surface consists mainly of oxides, oxyhydroxides, and hydroxides, which has been known to increase the adhesion of organic coatings [1] and may be an additional benefit to the cathode films in fabrication of Li-ion batteries. During long-term storage in the charged state or during charge–discharge cycling, however, pitting corrosion of the Al current collector has been observed in Li and Li-ion batteries [2–5], which is known to affect greatly the calendar life and cycling performance of the batteries. Pitting corrosion means that the Al surface is locally corroded to form many pin-like holes, and is easily determined by cyclic polarization measurements [6]. The potential at which the current starts to increase rapidly above the background current is referred to as a pitting potential (E_p). Al corrosion within the batteries will cause many problems: (i) it passivates the cathode active material, (ii) its solid products increase the electrical resistance, (iii) its soluble products contaminate the electrolyte and increase the self-discharge rate, and (iv) the dissolved Al^{3+} ions migrate to the counter anode and reductively deposit there. Therefore, many researchers have recently focused on the subject of identifying and solving the problem of Al corrosion in Li-ion batteries [7–14]. Most of the previous work addressed the Al stability with respect to the electrolyte solution at high potentials, which the cathode normally reaches during charge.

Several techniques have been employed to investigate the phenomenon of Al corrosion in the electrolyte solutions, such as cyclic voltammetry (CV) or linear sweep voltammetry (LSV) [11,12], electrochemical impedance spectroscopy (EIS) [10,11], X-ray photoelectron spectroscopy (XPS) [10], surface spectroscopy [10,11], electrochemical quartz crystal microbalance (EQCM) [12], and so forth. In the present work, we used LSV to compare the effect of the lithium salt and the electrolyte solvent on the Al corrosion, and we discuss the correlation of the oxidative potential and Al corrosion. The mechanism of Al corrosion is analyzed using EIS data and an attempt to suppress Al corrosion is made.

2. Experimental

Ethylene carbonate (EC, 99.95%, from Grant Chemical), $LiPF_6$ and $LiBF_4$ (both from Stella Chemifa Corp.) were used as received. While the solvents,1,2-dimethoxyethane

* Corresponding author. Tel.: +1-301-394-0046; 1-301-394-0273.
E-mail address: szhang@mail.com (S.S. Zhang).

0378-7753/02/$ – see front matter
PII: S0378-7753(02)00110-6

(DME, 99.5%, Aldrich) and dimethyl carbonate (DMC, 99%, Aldrich), were distilled over lithium chips, and the salts CF_3SO_3Li (3 M), $LiN(SO_2CF_3)_2$ (3 M), and $LiClO_4$ (Alfa Aesar), were dried at 120 °C for 24 h under vacuum before use. Using the above starting materials, electrolytes with different composition were prepared in an argon-filled glove box, which has both water and oxygen contents of less than 20 ppm. The electrolytes thus obtained usually had a water content of less than 25 ppm, as determined by the Karl–Fischer method. Lithium foil (Cypress–Foote Mineral) and Al wire (99.999%, 1.0 mm in diameter, Aldrich) were used as received.

Solartron Electrochemical Interface SI 1287 and Solartron Impedance/Gain-Phase Analyzer SI 1260, which were controlled by Corrware and Zplot software, were used to perform all electrochemical measurements. The test cell had a three-electrode configuration consisting of lithium foils as counter and reference electrodes, respectively. The working electrode was an Al wire that was wrapped by a thermally shrinkable Teflon tube with 1.0 cm length exposed to the electrolyte. After wrapping, the exposed area of Al wire was scratched using a knife so as to obtain a fresh surface. Cell assembly and electrochemical measurements were conducted in the same glove box as used in the preparation of electrolytes. The sweep rate in the LSV experimental was 5 mV/s and started from the open circuit voltage (OCV) of the newly assembled cell. The ac impedance was potentiostatically measured by applying a dc bias potential and an ac oscillation of 5 mV over the frequencies range 100 kHz to 0.01 Hz. Before the impedance measurement, the cell was potentiostatically polarized for 60 min at the potential that equals to the value of dc bias. The obtained EIS was analyzed by using ZView software (Scribner and Associates Inc.).

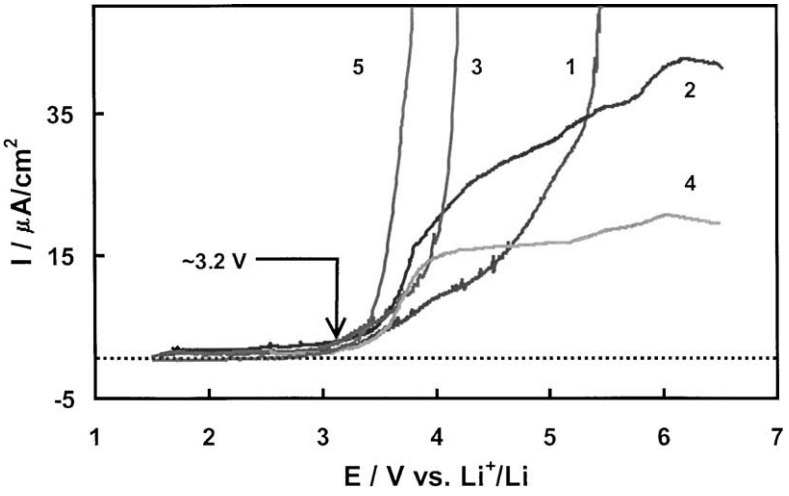

Fig. 1. *I–E* response of Al in 1:1 EC/DME solutions containing 1 M lithium salt, which was recorded from the first sweep at a sweep rate of 5 mV/s. (1) $LiClO_4$, (2) $LiPF_6$, (3) $LiN(SO_2CF_3)_2$, (4) $LiBF_4$, and (5) CF_3SO_3Li.

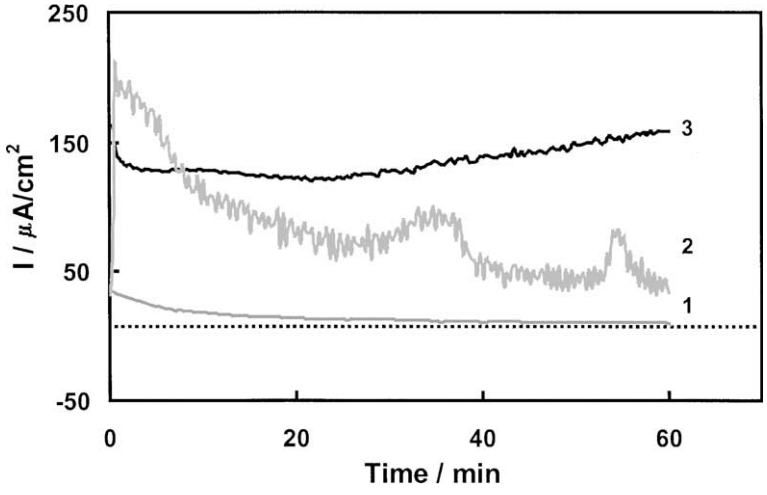

Fig. 2. Change of corrosion current with polarization time at 4.2 V vs. Li^+/Li in 1 M Li salt EC/DME solution, which was obtained from Al with newly scratched surface. (1) $LiPF_6$, (2) $LiClO_4$, and (3) CF_3SO_3Li.

3. Results and discussion

3.1. Effect of lithium salts

It is known that the water content substantially affects, the corrosion behavior of Al. To minimize this, we strictly controlled water content by drying starting materials before preparation of the electrolytes and made all measurements in a glove box. We first used a 1:1 (w/w) mixed solvent of EC and DME to evaluate the effect of Li salts on Al corrosion by a means of LSV. It should be mentioned that the OCV of a newly scratched Al in the electrolyte solutions was unstable and fluctuated between 2.5 and 0.5 V. Fig. 1 shows current response of Al to the potential in the EC/DME solution containing 1 M $LiClO_4$, $LiPF_6$, $LiN(SO_2CF_3)_2$, $LiBF_4$, or CF_3SO_3Li, respectively. It is observed that the corrosion current of Al rapidly increases around 3.2 V (hereafter called it as pitting potential, E_p), regardless of the supporting salts and electrolyte solvents. When the potential is higher than E_p, the current varies with the salt. In the solutions made of either $LiBF_4$ or $LiPF_6$, the current at the higher potentials is significantly suppressed. This means that the Al surface has been effectively passivated, which protects it from being further oxidized. While in the solutions containing $LiClO_4$, CF_3SO_3Li, or $LiN(SO_2CF_3)_2$, respectively, the current increases continuously and Al shows increased dissolution with the potential. In these cases, the corrosion current is too large to be fully displayed in the figure. Among the tested electrolytes, the least corrosion is observed from $LiBF_4$, while the worst corrosion from CF_3SO_3Li. This observation may be ascribed to the different solubility of the Al corrosion products. After experiments in CF_3SO_3Li solution, we found that Al was severely pitted (corroded) and many black and loose precipitates were formed on the surface of Li counter electrode. We noticed that the appearance of these back precipitates found on the Li surface differ from that of the deposited metal lithium, as observed in a normal Li deposit experiment. We consider that these precipitates are likely Li–Al alloy or Li/Li–Al alloy mixture because under electrical field, the dissolved Al^{3+} ions may migrate across the electrolyte to the counter Li electrode and reductively deposit there in a form of Li–Al alloy. It is shown in Fig. 1 that the stability of Al with respect to the anodic polarization increases in an order of $CF_3SO_3Li < LiN(SO_2CF_3)_2 < LiClO_4 < LiPF_6 < LiBF_4$.

Fig. 2 plots the time dependence of the corrosion current of Al at the polarization potential of 4.2 V in EC/DME solutions containing CF_3SO_3Li, $LiClO_4$, or $LiPF_6$, respectively. In $LiPF_6$ solution, the anodic current of Al gradually decreased, indicating that both Al and solvents are stable, while the anodic current in CF_3SO_3Li solution constantly remained above 120 μA/cm^2 and it accompanied a continuous dissolution of Al. After polarization test in the CF_3SO_3Li solution, we observed that Al was severely corroded and many corrosion products precipitated near Li counter electrode and at the bottom of the cell. The anodic current of Al in $LiClO_4$ solution behaved in rather a complicated manner with a generally declining trend. The anodic current was unstable with erratic fluctuations and board peaks. This suggests that the passive layer formed with $LiClO_4$ solution may be not stable enough and it may occasionally break down.

3.2. EIS change with potential

Fig. 3 displays Nyquist plots of Al at various polarization potentials in 1:1 EC/DME solutions containing 1 M either $LiPF_6$ or CF_3SO_3Li. The profile of the EIS greatly varies with the polarization potential, which may be generally

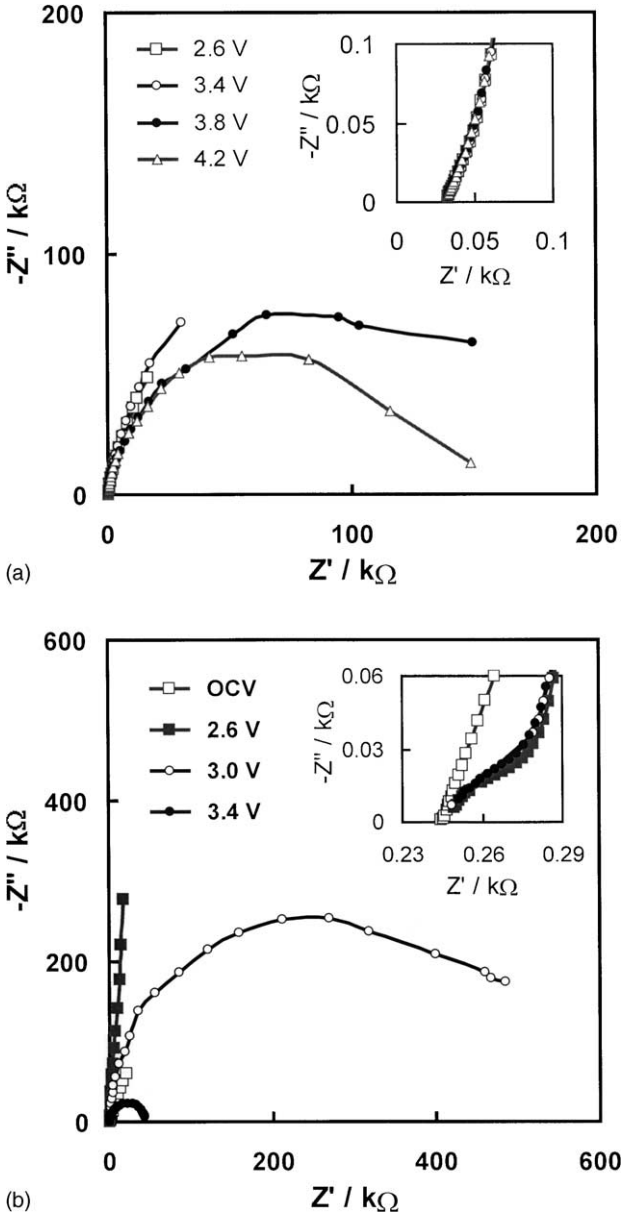

Fig. 3. Nyquist plots of Al in 1 M Li salt 1:1 EC/DME solution under various polarization potentials. Inset is the part of EIS at high frequency. (a) $LiPF_6$ and (b) CF_3SO_3Li.

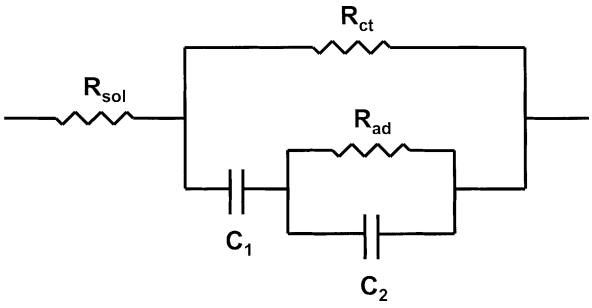

Fig. 4. Equivalent circuit used to analyze the corrosion process of Al.

analyzed using an equivalent circuit as shown in Fig. 4 [15,16]. R_{sol} is the resistance of electrolyte solution, R_{ct} and C_1 are the charge-transfer resistance and double-layer capacitance, respectively. R_{ad} and C_2 are the resistance and capacitance associated with the adsorbed layer on the Al surface. This equivalent circuit has been used by many authors to describe the electrochemical process of metal corrosion in aqueous solutions and in non-aqueous electrolytes [10,15–17]. In accordance with the literature [15,16], the electrochemical process of Al corrosion can be described in these two steps:

$$Al \rightarrow Al^{3+} + 3e^- \quad (1)$$

$$Al^{3+} + X^- \rightarrow AlX^{2+}_{(ads)} \text{ or } AlX^{+}_{2(ads)} \text{ and } AlX_{3(ads)} \quad (2)$$

In the EIS, the semicircle at high frequency corresponds to step 1 (as reflected by R_{ct} and C_1), while the one at low frequency regions corresponds to step 2 (as reflected by R_{ad} and C_2). The R_{ct} is related to an exchange current (i^0) by the equation [18]:

$$R_{ct} = \frac{RT}{nFi^0} \quad (3)$$

where R is the gas constant, F the Faraday constant, and n the number of electrons involved in the electrochemical process. In general, the higher R_{ct} reflects a lower Al corrosion since the exchange current is directly associated with the electrochemical process of Al corrosion. Similarly, the higher R_{ad}

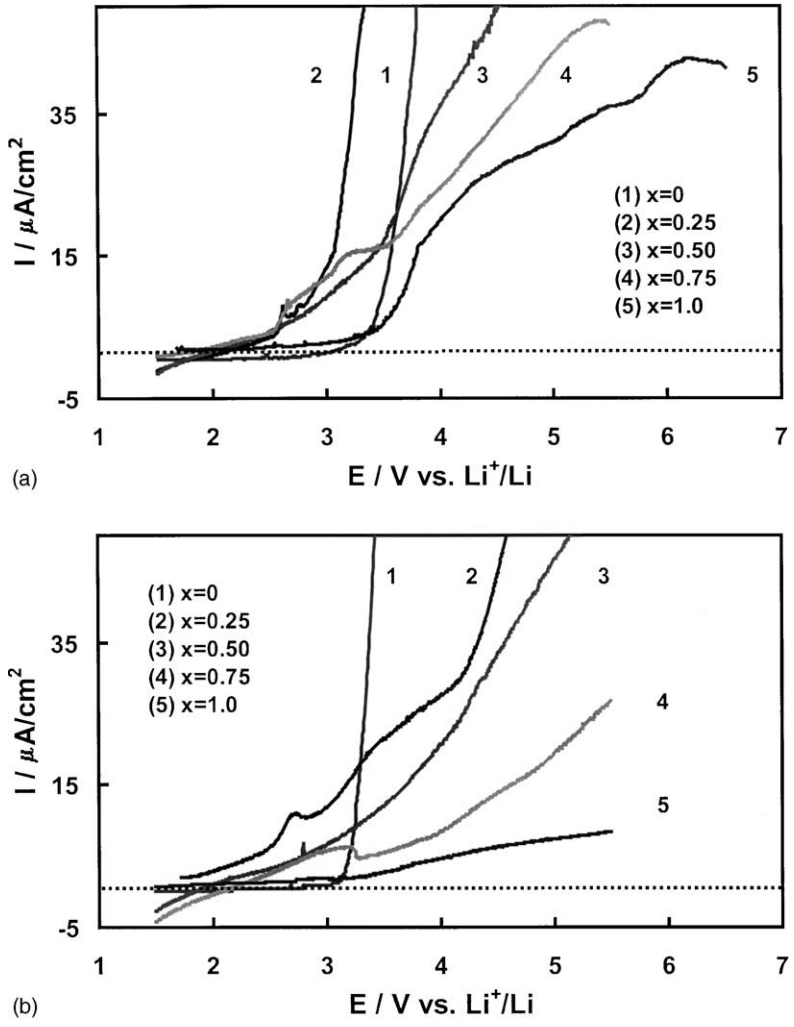

Fig. 5. *I–E* response of Al in 1 M $(1-x)CF_3SO_3Li$–$xLiPF_6$ mixed salt solutions, which was recorded from the first sweep at a sweep rate of 5 mV/s. (a) 1:1 EC/DME and (b) 1:1 EC/DMC.

corresponds to lower corrosion, which may be ascribed to good adhesion of the adsorbed (passive) layer to the Al surface.

Fig. 3a shows that Al has a high R_{ct}, which explains the fact that Al is less corroded in $LiPF_6$ solution. At the potentials of below 3.4 V, EIS of Al is a nearly straight slope line. This means that the R_{ct} is very high and no corrosion takes place in these potential regions. When the potential is increased to 3.8 V, a semicircle with a large R_{ct} appears. With further increase in the potential, the corrosion is aggravated, as indicated by a decreased R_{ct} (compare EIS at 3.8 and 4.2 V). On the other hand, Al corrosion behaves differently in the CF_3SO_3Li solution. At the OCV of the newly assembled cell, the EIS is a straight slope line (see Fig. 3b and its inset), showing no corrosion. When the potential is increased to 2.6 V or higher, the semicircle at high frequency appears. The value of R_{ct} is evaluated from the inset of Fig. 3b to be in a range of only tens of ohms, which indicates severe corrosion. When the potential is further increased, the second semicircle (corresponding to R_{ad}) at the low frequency end appears. Furthermore, the value of R_{ad} is decreased with the potential. The decreased R_{ad} at the higher potentials might imply that the dissolution products of Al cannot tightly adhere to the Al surface. The higher potential leads to worsened Al corrosion.

3.3. Effect of mixed salts

Fig. 5a compares the current response of Al to the polarization potential in 1:1 EC/DME solutions containing 1 M mixed salt of CF_3SO_3Li and $LiPF_6$. We observed that combinations of these two salts increases the E_p and aggravates Al corrosion at potentials of 2.5–3.0 V. It is also shown that the combination of two salts leads to the E_p decreasing from original 3.2 to ~2.5 V. When the content of $LiPF_6$ is less than 75%, addition of $LiPF_6$ into CF_3SO_3Li cannot suppress Al corrosion current.

Similar phenomena were observed in 1:1 EC/DMC mixed solvent (Fig. 5b). There is no obvious difference in the *I–E* response of Al corrosion between EC/DME and EC/DMC mixed solvents. A small difference is that the corrosion was better suppressed in EC/DMC solvent at the potentials of above E_p when the content of $LiPF_6$ was more than 75%. This may be due to that Al form a more stable passive layer in EC/DMC solvent. However, the observed effect of solvents is too small to affect Al corrosion. From the results described earlier, one may conclude that the electrolyte solvent has negligible impact on the Al corrosion, while the combination of two salts aggravates Al corrosion.

3.4. Effect of pre-existing passive layer

To determine if the pre-existing passive layer can protect Al, we treated Al at 480 °C in air for 24 h. Such a treatment is supposed to pre-form an oxide-based passive layer on the Al surface and to help Al resist corrosion. To test this, we selected $LiClO_4$ solution because it is not as corrosive to Al as CF_3SO_3Li solution. Fig. 6 compares EISs of the Al without and with oxidation pretreatment in 1 M $LiClO_4$ 1:1 EC/DME electrolyte. The EIS of the newly scratched Al consists of an incomplete semicircle (Fig. 6a). At the high frequency end, the semicircle crosses at 0.032 kΩ with the Z' axis (see inset of Fig. 6a). This value reflects the resistance of the electrolyte solution and is independent of the polarization potentials. However, the semicircle's diameter (i.e. the R_{ct}) decreases with higher polarization potentials. This behavior is very similar to that observed in the CF_3SO_3Li and $LiPF_6$ solution, which is a characteristic of corrosion.

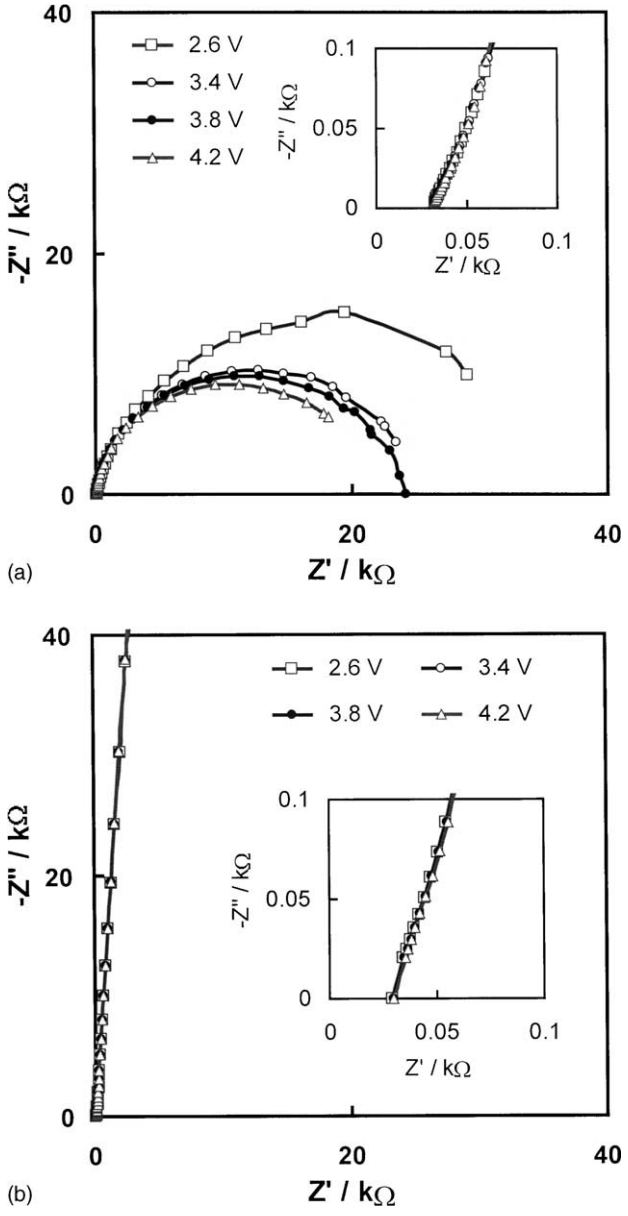

Fig. 6. Nyquist plots of Al in 1 M $LiClO_4$ 1:1 EC/DME solution under various polarization potentials, in which the inset is the part of EIS in the high frequency region: (a) newly scratched Al, and (b) pretreated Al by heating it at 480 °C in air for 24 h.

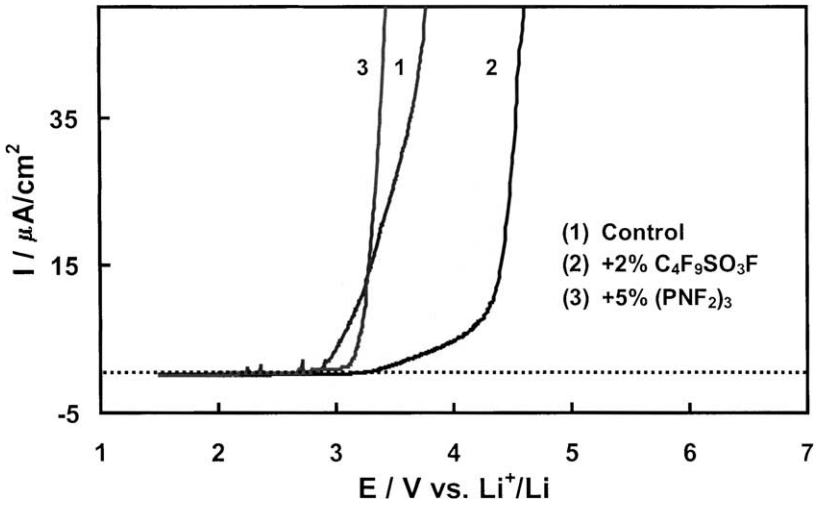

Fig. 7. Effect of electrolyte additive on the *I–E* response of Al in 1 M CF_3SO_3Li 1:1 EC/DMC solution, which was recorded from the first sweep at a sweep rate of 5 mV/s. (1) Control electrolyte, (2) with 2 wt.% of $C_4F_9SO_2F$, and (3) with 5 wt.% of $(PNF_2)_3$.

Fig. 6b exhibits that EISs of the oxidation pretreated Al are only a straight line without the semicircles. The inset of Fig. 6b shows the same resistance of the electrolyte solution as that obtained from the EIS of the scratched Al. The difference in the EISs between Fig. 6a and b reveals that the pre-existing passive layer on the Al surface can effectively help Al resist corrosion. Unfortunately, it has been found that the pre-existing passive layer could not protect Al from pitting corrosion in a Li battery upon long-term storage [5].

3.5. Effect of electrolyte additive

To understand the fact that $LiPF_6$-based electrolyte is less corrosive to Al, we attempted to examine the effect of additives on Al corrosion. Behl et al. [8,9] reported that fluorides in $LiPF_6$ and $LiBF_4$ are helpful in stabilizing Al in Li-ion battery electrolytes, while other work [10] revealed that Li and P are the predominant adsorbed species on the Al surface in $LiPF_6$-based electrolyte. To examine the effect of F and P on the Al corrosion, we studied the compounds, which may disassociate into F or P species, as an electrolyte additive. For this purpose, perfluoro-1-butanesulfonyl fluoride ($C_4F_9SO_2F$ in which SO_2F is active, 96%, Aldrich) was selected as an active F source and phosphonitrilic fluoride trimer ($(PNF_2)_3$, 99%, Aldrich) for both active F and P sources. The effect of these two additives on the Al corrosion in 1 M CF_3SO_3Li 1:1 EC/DMC electrolyte is illustrated in Fig. 7. The E_p of Al is evaluated to be 2.96, 3.13, and 3.43 V in the control electrolyte, 2 wt.% of $C_4F_9SO_2F$, and 5 wt.% of $(PNF_2)_3$, respectively. However, these two additives cannot suppress the corrosion current at the higher potentials, at which severe corrosion of Al still takes place. This fact suggests that the stabilization of Al by $LiPF_6$ may be in a more complicated means than a simple reaction with the active F or P.

4. Conclusions

In conclusion, pitting corrosion of Al in the electrolytes of Li and Li-ion battery takes place at ~3.2 V versus Li^+/Li, independent of the salts and solvents. The Li salt substantially affects the corrosion behavior of Al. Insolubility in the electrolyte and good adhesion to the Al surface of the corrosion products are critical for the formation of a stable passive layer. In the EIS, Al corrosion can be described by an equivalent circuit consisting of a charge-transfer resistance (R_{ct}) and an adsorbed layer resistance (R_{ad}). The high R_{ct} corresponds to a slow electrochemical process of the Al corrosion, while the high R_{ad} corresponds to a stable passive layer. Among the examined Li salts, we observed that the stability of Al at potentials of above 3.2 V increases in an order of $CF_3SO_3Li < LiN(SO_2CF_3)_2 < LiClO_4 < LiPF_6 < LiBF_4$. Coexistence of two salts, such as CF_3SO_3Li and $LiPF_6$, decreases the pitting potential and aggravates Al corrosion. Compounds containing active fluoride may increase the pitting potential but cannot suppress Al corrosion at higher potentials.

Acknowledgements

We thank Dr. M.S. Ding and Dr. K. Xu for their help in the ac impedance measurements and for valuable discussions, respectively.

References

[1] S. Lopez, J.P. Petit, H.M. Dunlop, J.R. Butruille, G. Tourillon, J. Electrochem. Soc. 145 (1988) 823.
[2] E.M. Shembel, R.D. Apostolova, A.S. Strizhko, A.I. Belosokhov, A.F. Naumenko, V.V. Rozhkov, J. Power Sources 54 (1995) 421.

[3] J. Braithwaite, S. Lucero, W. Cieslak, G. Nagasubramanian, ECS Meeting Abtracts, Vol. 96-2, Boston, MA, 1996, p. 64.
[4] X. Zhang, P.N. Ross, J.R. Kostecki, F. Kong, S. Sloop, J.B. Kerr, K. Striebel, E.J. Cairns, F. McLarnon, J. Electrochem. Soc. 148 (2001) A463.
[5] S.S. Zhang, M.S. Ding, T.R. Jow, J. Power Sources 102 (2001) 16.
[6] G.S. Frankel, J.R. Scully, C.V. Jahnes, J. Electrochem. Soc. 143 (1986) 1834.
[7] L.J. Krause, W. Lamanna, J. Summerfield, M. Engle, G. Korba, R. Loch, R. Atanasoski, J. Power Sources 68 (1997) 320.
[8] W.K. Behl, E.J. Plichta, J. Power Sources 72 (1998) 132.
[9] W.K. Behl, E.J. Plichta, J. Power Sources 88 (2000) 192.
[10] J.W. Braithwaite, A. Gonzales, G. Nagasubramanian, S.J. Lucero, D.E. Peebles, J.A. Ohlhausen, W.R. Cieslak, J. Electrochem. Soc. 146 (1999) 448.
[11] Y. Chen, T.M. Devine, J.W. Evans, O.R. Monteiro, I.G. Brown, J. Electrochem. Soc. 146 (1999) 1310.
[12] H. Yang, K. Kwon, T.M. Devine, J.W. Evans, J. Electrochem. Soc. 147 (2000) 4399.
[13] X. Wang, E. Yasukawa, S. Mori, Electrochim. Acta 45 (2000) 2677.
[14] J. Kawakita, K. Kobayashi, J. Power Sources 90 (2000) 182.
[15] J.P. Diard, J.M. LeCanut, B. LeGorrec, C. Montella, Electrochim. Acta 43 (1998) 2469.
[16] R. Casparac, C.R. Martin, E.S. Lisac, Z. Mandic, J. Electrochem. Soc. 147 (2000) 991.
[17] R.G. Buchheit, M. Cunningham, H. Jensen, M.W. Kendig, Corrosion 54 (1998) 61.
[18] A.J. Bard, L.R. Faulkner, Electrochemical Methods, Fundamentals and Applications, Wiley, New York, 1980 (Chapters 3 and 9).